A GenoChemetic strategy for derivatization of the violacein natural product scaffold

Hung-En Lai[1#], Alan M. C. Obled[4], Soo Mei Chee[1,3], Rhodri M. Morgan[2], Rosemary Lynch[4], Sunil V. Sharma[4], Simon J. Moore[1^], Karen M. Polizzi[5], Rebecca J. M. Goss*[4], Paul S. Freemont*[1,3, 6]

[1]Section of Structural and Synthetic Biology, Department of Infectious Disease, Imperial College London, London SW7 2AZ, UK.
[2]Department of Life Sciences, Imperial College London, London SW7 2AZ, UK.
[3]London Biofoundry, Imperial College Translation & Innovation Hub, London, W12 0BZ, UK
[4]School of Chemistry and Biomedical Sciences Research Complex, University of St Andrews, North Haugh, St Andrews, Fife, KY16 9ST, UK.
[5]Department of Chemical Engineering, Imperial College London, London SW7 2AZ, UK.
[6]UK DRI Care Research and Technology Centre, Imperial College London, Hammersmith Campus, Du Cane Road, London, W12 0NN, UK.

*Correspondence: rjmg@st-andrews.ac.uk; p.freemont@imperial.ac.uk
^current address School of Biosciences, University of Kent, Canterbury, CT7 2NJ
#current address School of Biological Sciences, Victoria University of Wellington, Wellington 6011, New Zealand.

Lead Contact: p.freemont@imperial.ac.uk

Keywords

Violacein, antibiotics biosynthesis, natural product analogue, rebeccamycin, bisindole, halogenase, cross-coupling, GenoChemetics

Abstract

Natural products and their analogues are often challenging to synthesise due to their complex scaffolds and embedded functional groups. Solely relying on engineering the biosynthesis of natural products may lead to limited compound diversity. Integrating synthetic biology with synthetic chemistry allows rapid access to much more diverse portfolios of xenobiotic compounds which may accelerate the discovery of new therapeutics. As a proof-of-concept, by supplementing an *Escherichia coli* strain expressing the violacein biosynthesis pathway with eight tryptophan substrate analogues or tryptophan halogenase RebH *in vivo*, 68 new-to-nature analogues of violacein were generated, demonstrating extraordinary promiscuity of the violacein biosynthesis pathway. Furthermore, 20 new derivatives were generated from brominated violacein analogues via Suzuki-Miyaura cross-coupling reaction directly using the crude extract without prior purification. Herein, we demonstrate a flexible and rapid approach

to access diverse chemical space that can be applied to a wide range of natural product scaffolds.

Introduction

Total synthesis of natural products and their analogues has often been challenging and costly due to their structural complexities (Kirschning and Hahn, 2012). However, greater chemical space may be accessed through utilisation of synthetic chemistry methodologies and reagents compared to employing enzyme-catalysed biosynthesis alone. Combining biosynthesis with chemical synthesis represents a powerful approach for rapidly generating new analogues of complex natural products and libraries of chemical derivatives suitable for screening and structure-activity relationship (SAR) assays (Eichner et al., 2012; Goss et al., 2012), leading to discovery of new and more potent compounds. The generation of such analogues can enable improvement in bioactivity and bioavailability, as illustrated, for example, by analogues of the 'last-resort' antibiotic vancomycin, with >200-fold improvement of potency compared to vancomycin in resistant *Enterococci* strains (Okano et al., 2017). In another study, the addition of a sterically unhindered primary amine group to a Gram-positive antibiotic deoxynybomycin expanded its antimicrobial activity to multi-drug-resistant Gram-negative pathogenic strains (Richter et al., 2017).

As a proof-of-concept, we have focused on the violacein biosynthetic pathway. Violacein (**1**), a violet pigment first isolated from the bacterium *Chromobacterium violaceum*, is part of the bisindole biosynthetic family that utilises L-tryptophan as the starting substrate. The violacein pathway is encoded within a conserved operon of five genes (*vioABCDE*), whose gene products catalyse a 14-electron oxidative biosynthesis pathway (Balibar and Walsh, 2006). The bisindole biosynthetic pathways have attracted considerable interest because of their therapeutic potential for medical applications, including antimicrobial, antiviral, trypanocidal and antitumorigenic properties (Durán et al., 2012). The violacein biosynthetic pathway also produces deoxyviolacein (**2**) as a by-product, and the coloured properties of violacein and deoxyviolacein make them interesting targets for natural product pathway

engineering, such as promoter library screening (Jones et al., 2015), CRISPR-based multiplex transcriptional regulation (Zalatan et al., 2015) or diverting pathway flux via RBS engineering (Jeschek et al., 2016).

A study on oxyviolacein, a hydroxylated analogue of violacein generated by feeding exogenous 5-hydroxy-L-tryptophan (Hoshino and Ogasawara, 1990), showed bioactivity against a collection of pathogenic bacteria and fungi strains (Wang et al., 2012) suggesting that violacein analogues may be a good starting point for developing more potent antibiotics. A similar rationally designed precursor-directed biosynthetic strategy has also showed considerable success in generating analogues of flavonoids (Kufs et al., 2020). Other examples of using altered biosynthetic pathways for analogue generation, include using various enzyme homologues from bisindole pathways (Du and Ryan, 2015; Sánchez et al., 2005), interconversion of the biosynthetically related novobiocin and clorobiocin aminocoumarin antibiotics (Eustáquio et al., 2004), introduction of the halogenase from hormaomycin pathway to generate clorobiocin analogues (Heide et al., 2008), the generation of chlorinated monoterpene indole alkaloids (Runguphan et al., 2010), and chlorinated and brominated analogues of the antibiotic pacidamycin (Deb Roy et al., 2010). Although total chemical synthesis of violacein (Petersen and Nielsen, 2013; Wille and Steglich, 2001) and some substituted analogues (Haun et al., 1992; McLaughlin et al., 2014) have been reported, these syntheses are challenging and low yielding. Pathway manipulation could represent a more flexible, sustainable and rapid approach for generating violacein analogues. In this study, we have applied such approaches to generate 88 new violacein or deoxyviolacein analogues via a combination of pathway engineering enabling enzymatic halogenation of the starting substrate tryptophan, feeding different substrate analogues, and further derivatization using Suzuki-Miyaura cross-coupling directly in crude extracts (**Figure 1**).

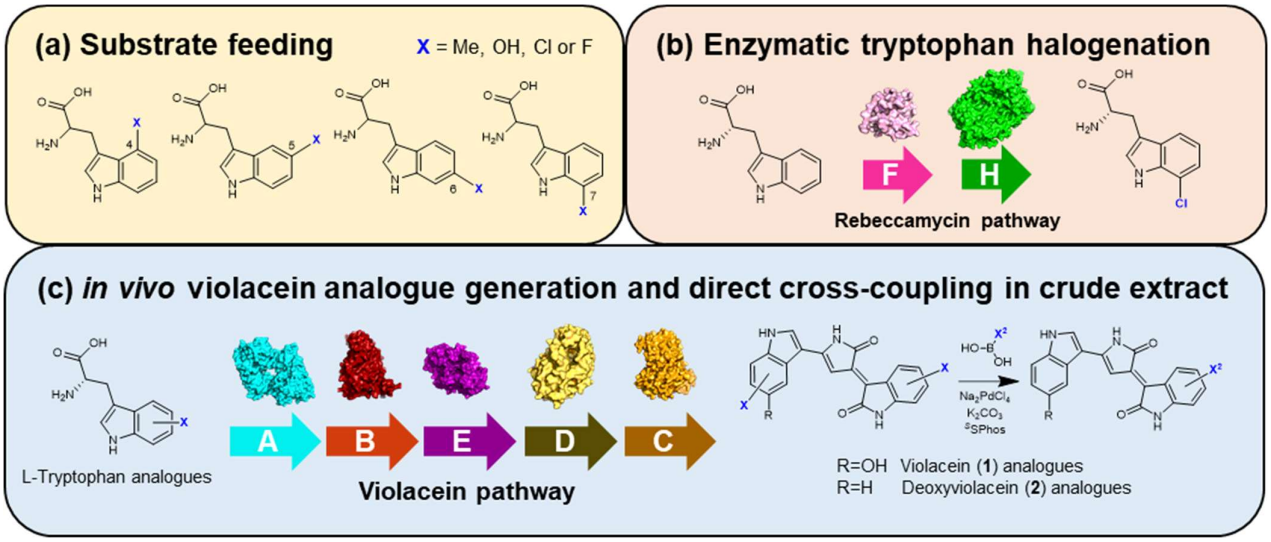

Figure 1. Schematics of GenoChemetic approach used in this study. Analogues of violacein (**1**) or deoxyviolacein (**2**) can be generated by either feeding synthetic tryptophan analogues to *E. coli* cells expressing the violacein biosynthesis pathway VioABCDE, or *in vivo* halogenation of tryptophan by expressing flavin reductase RebF and tryptophan halogenase RebH with the rest of violacein pathway. Further derivatization via Suzuki-Miyaura cross-coupling lead to new synthetic analogues. Available enzyme structures are shown and correspond to VioA, (PDB 6G2P); VioD (PDB 3C4A); VioE (PDB 3BMZ); RebH (PDB 2E4G) as well as models generated *in silico* by Phyre2 (http://www.sbg.bio.ic.ac.uk/phyre2) for VioB, VioC and RebF.

Results and Discussion

VioA, the first enzyme in the violacein biosynthesis pathway, oxidises the substrate L-tryptophan to form the first pathway intermediate indole-3-pyruvic acid imine (IPA imine). In order to determine whether VioA would accept different tryptophan analogues as substrates, we purified VioA and carried out VioA enzyme kinetic assays against various substrate analogues including L-tryptophan (TRP), 4-fluoro-DL-tryptophan (4FT), 5-methyl-DL-tryptophan (5MeT), 6-fluoro-DL-tryptophan (6FT) and 7-methyl-DL-tryptophan (7MeT) (**Figure S1**). The kinetics of VioA against L-tryptophan (k_{cat} = 3.04 ± 0.67 s^{-1}, K_M = 447 ± 156 μM) have been previously determined with both UV-monitored substrate depletion and coupled peroxidase assays, although only the kinetic data generated from the substrate depletion assay was reported (k_{cat} = 3.38 ± 0.32 s^{-1}, K_M = 31 ± 11 μM) (Balibar and Walsh, 2006). The discrepancy between the reported values and our data could be due to the difference in assay conditions, and the multiple reaction steps involved in coupled peroxidase assay. We also observed approximately 76% higher activity of VioA against 5MeT (k_{cat} = 5.94 ± 2.84 s^{-1}, K_M = 511 ± 94

μM) compared to TRP, in agreement with a previous characterisation study which assumed Michaelis-Menten kinetics (Füller et al., 2016). In the same study, the authors also solved the structure of VioA complexed with a competitive inhibitor 2-[(1H-indol-3-yl)methyl]prop-2-enoic acid (IEA) (PDB **5G3U**)[2], and generated a collection of VioA active site mutants to probe their substrate promiscuity. However, these VioA mutants exhibited decreased activity with most tryptophan analogues tested compared to wild-type VioA, demonstrating the difficulty in rationally engineering VioA towards increased substrate promiscuity (Füller et al., 2016). Another study reported the structure of VioA C395A mutant (PDB accession **5ZBD**) which demonstrated improved thermostability but no significantly improved activity (Yamaguchi et al., 2018). To date, there has been no wild-type VioA structure complexed with the native substrate tryptophan or its substituted analogues.

To determine if the substrate kinetics differences were due to alterations in substrate binding, we next solved the crystal structures of VioA complexed with TRP (PDB **6G2P**), 4FT (PDB **6FW7**), 5MeT (PDB **6FW8**), 6FT (PDB **6FW9**) and 7MeT (PDB **6FWA**) with resolutions ranging from 2.4 Å to 3.0 Å (**Figure 2A, 2B**, data statistics in **Table S1**). The active site of VioA reveals several key residues surrounding the C4- to C7-positions of tryptophan substrate indole ring. Of the four positions, C4 and C7 have the most space around the binding site pocket compared to C5 and C6 due to Asp311 and Ala145 side chains (**Figure 2A**), suggesting that VioA would have the lowest affinity for tryptophan analogues with substituent groups at the C5- and C6-positions. However, the interatomic distances between respective Cα atom or amine nitrogen atom and N5 of FAD cofactor is conserved for all the analogues (between 3.93 Å to 4.69 Å for Cα atom, 3.62 Å to 5.63 Å for amine nitrogen) and is similar to the TRP-bound structure (3.93 Å for Cα atom and 5.07 Å for amine nitrogen) (**Figure S2**). This showed that all the analogues can bind VioA in a catalytically active, but slightly different conformation. Interestingly, the hydrogen bonding between Arg64 and Tyr309 and the carboxylate group of all substrate analogues are conserved, as are the positions of the other active site residues (**Figure 2B**). Of the four structures with tryptophan analogues, 4FT-bound

VioA structure has the lowest resolution at 3.0 Å and weakest density around the 4FT ligand compared to the other structures (**Figure S2**), suggesting lower occupancy binding which also correlates with the observed poorer enzyme kinetics compared to TRP. In addition, we observe two alternative conformers for the bound 6FT ligand demonstrating further conformational flexibility of tryptophan analogue binding. In summary, our structural analyses show that a variety of tryptophan analogues can bind VioA in different conformations, although the positions of active site residues and associated hydrogen bonding patterns are similar to TRP-bound VioA. Our data clearly show that the VioA active site can flexibly accommodate a variety of tryptophan substrate analogues for catalysis.

Having determined that VioA accepts various tryptophan analogues, we next investigated the potential for derivatizing violacein using a substrate feeding approach, using commercially available tryptophan analogues as starting precursors. This included 4-fluoro-, 5-fluoro-, 6-fluoro-, 5-chloro-, 5-hydroxyl-, 6-methyl- and 7-methyl-substituted tryptophan analogues. By adding the tryptophan analogues to cultures of *E. coli* cells that were expressing a synthetic violacein biosynthesis pathway *vioABCDE* (**Figure 2C**), a total of 62 new compounds were observed including structural isomers due to the asymmetry of the violacein core scaffold, demonstrating promiscuity of violacein biosynthesis enzymes (**Figure S3**). The percentage compositions of the various violacein and deoxyviolacein analogues were calculated based on the extracted total ion chromatogram (TIC) peak area obtained from LC-HRMS/MS analyses (**Table S2**, **Figure 2D**). The slow kinetics of 4FT with VioA may contribute to the least violacein analogue conversion, suggesting that VioA may be the rate-limiting step for generating violacein analogues from the pathway, although this would require further studies to investigate the relative rates of pathway intermediates in each of the enzymatic steps of the pathway.

We then assayed the growth inhibitory activity of the crude violacein extracts containing the various analogues and a control containing only the underivatized scaffolds against *Bacillus*

subtilis cultures as a Gram-positive model organism. Using crude extracts of violacein analogues we observed few changes in growth inhibition compared to the extracts containing unmodified crude violacein (**Figures S4**). Interestingly, the 6MeT extract has about 4-fold higher IC50 compared to the 7MeT extract, where the only difference between these two samples is the position of methyl group attached to the indole ring, suggesting that the C6 substitution might be important for activity. In addition, cell extracts containing only deoxyviolacein did not show any significant inhibition towards *B. subtilis*, suggesting that the 5-hydroxyl group of violacein confers the antimicrobial activity, in agreement with previous studies (Bilsland et al., 2018; Jiang et al., 2012; Wang et al., 2012). More recently, we tested crude violacein extracts containing mixtures of substituted analogues in a growth assay for the malarial parasite *Plasmodium falciparum*, and found a wide ranging of inhibitory activity at 0.5 μM, with some analogues comparable to that of the positive control cycloheximide (Wilkinson et al., 2020). This indicates that further testing of violacein extracts biosynthesised from *E. coli* against other pathogens of interest could lead to discovery of compounds with therapeutic potential.

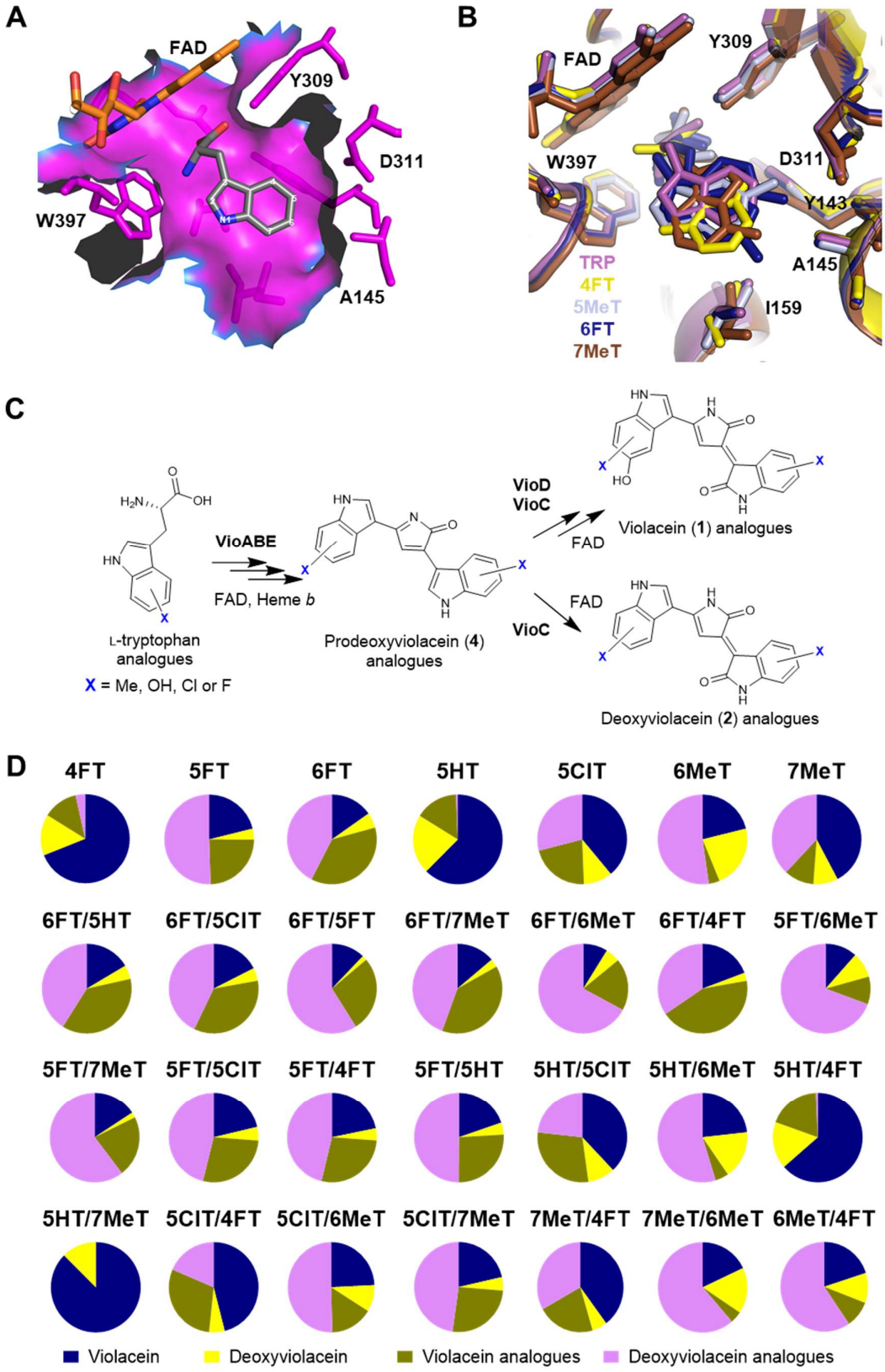
A
FAD
Y309
D311
W397
A145
B
FAD
Y309
W397
D311
Y143
A145
I159
TRP
4FT
5MeT
6FT
7MeT
C
VioABE
FAD, Heme b
L-tryptophan analogues
X = Me, OH, Cl or F
Prodeoxyviolacein (4) analogues
VioD
VioC
FAD
Violacein (1) analogues
VioC
FAD
Deoxyviolacein (2) analogues
D
4FT
5FT
6FT
5HT
5CIT
6MeT
7MeT
6FT/5HT
6FT/5CIT
6FT/5FT
6FT/7MeT
6FT/6MeT
6FT/4FT
5FT/6MeT
5FT/7MeT
5FT/5CIT
5FT/4FT
5FT/5HT
5HT/5CIT
5HT/6MeT
5HT/4FT
5HT/7MeT
5CIT/4FT
5CIT/6MeT
5CIT/7MeT
7MeT/4FT
7MeT/6MeT
6MeT/4FT
Violacein
Deoxyviolacein
Violacein analogues
Deoxyviolacein analogues

Figure 2. VioA structure and generation of violacein and deoxyviolacein analogues via substrate feeding. **(A)** Binding site pocket showing space enclosed by residues (magenta) around L-tryptophan (grey with elemental colour). The carbon positions of tryptophan indole ring are labelled. **(B)** Superimposition of active sites of VioA structures complexed with L-tryptophan (TRP, magenta), 4-fluoro-L-tryptophan (4FT, yellow), 5-methyl-L-tryptophan (5MeT, light grey), 6-fluoro-Ltryptophan (6FT, dark blue) and 7-methyl-L-tryptophan (7MeT, brown) in stick representation. Side chains surrounding the tryptophan ligand are labelled. Note that 6FT has 2 conformers fitted in the density map (see **Figure S2**). **(C)** Schematics of substrate feeding leading to analogues generation. **(D)** Compositions of violacein (**1**), deoxyviolacein (**2**), violacein analogues and deoxyviolacein analogues based on extracted TIC peak area of LC-HRMS/MS analyses of crude extracts of *E. coli* cells fed with either a single type, or a combination of two types of, substituted tryptophan substrate analogues. 4FT, 4-fluoro-DL-tryptophan; 5FT, 5-fluoro-DL-tryptophan; 6FT, 6-fluoro-DL-tryptophan; 5HT, 5-hydroxy-L-tryptophan; 5ClT, 5-chloro-DL-tryptophan; 6MeT, 6-methyl-DL-tryptophan; 7MeT, 7-methyl-DL-tryptophan.

Due to the promiscuity of the enzymes involved in the biosynthesis of violacein, we rationalized that a combination of enzymes from closely related bisindole biosynthesis pathways could generate compatible tryptophan analogues leading to other interesting new-to-nature analogues of violacein that might be otherwise difficult to synthesise. Rebeccamycin is a closely related bisindole where the biosynthetic pathway contains several genes including *rebO* and *rebD* which are homologous to *vioA* and *vioB* respectively. In addition, the pathway also consists of a tryptophan 7-halogenase RebH and its associated flavin reductase RebF that are responsible for generating 7-chloro-L-tryptophan from L-tryptophan via a chloraminelysine intermediate (Yeh et al., 2005, 2007). As a proof-of-principle, we combined the rebeccamycin (Reb) and violacein (Vio) biosynthetic operons using the Golden Gate cloning kit EcoFlex (Lai et al., 2018; Moore et al., 2016) in order to generate C7-chlorinated violacein analogues, which we were able to successfully produce in *E. coli* cells (**Figure 3A, 3B**) identified via LC-HRMS/MS (**Figure 3C**, **Table S2**). We found that although the RebOD+VioCDE strain (lacking RebFH) did not produce any chlorinated analogues of violacein, it was able to functionally substitute VioAB to produce violacein and deoxyviolacein (Balibar and Walsh, 2006). Next, by comparing RebFH+VioABCDE and RebFHOD+VioCDE (where RebOD replaced VioAB) strains, we observed that RebOD increased the proportion of chlorinated analogues from 6% to 33% when compared with VioAB (**Figure 3D, 3E**). This was likely due to the fact that RebO has k_{cat}/K_m value 57-times higher for 7-Cl-L-tryptophan than that of L-tryptophan (Nishizawa et al., 2006), thus RebO and RebD preferentially accept the 7-

chloro analogue of L-tryptophan and IPA imine respectively, producing the 7-chlorinated intermediate for downstream enzymes in the violacein biosynthesis pathway. By replacing the weak promoter J23114 for RebF and RebH with a medium strength promoter J23108, we also observed a total analogue increase of nearly 30% (**Figure 3F**). This shows that it is possible to fine tune the proportion of chlorinated analogue by changing the promoter strength of pathway enzymes, and optimization of fermentation protocols such as length of incubation, temperature, media conditions might further increase both proportion and the total amount of chlorinated analogues (Jones et al., 2015).

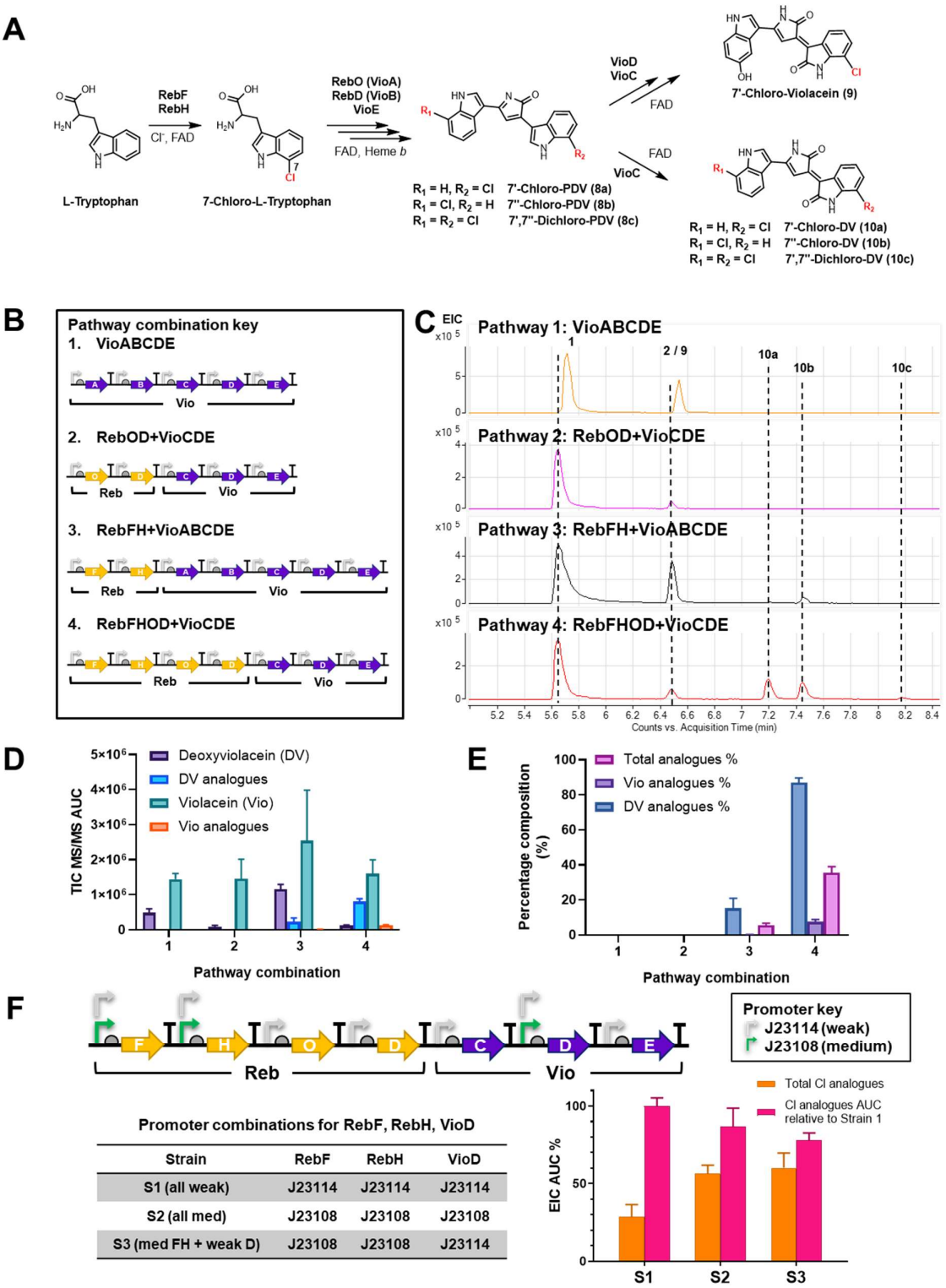

Strain	RebF	RebH	VioD
S1 (all weak)	J23114	J23114	J23114
S2 (all med)	J23108	J23108	J23108
S3 (med FH + weak D)	J23108	J23108	J23114

Figure 3. Generation of 7-chloro analogues of violacein and deoxyviolacein via in vivo halogenation. **(A)** Schematic of the hybrid rebeccamycin-violacein pathway enzymes that lead to 7-chloro analogues of violacein (**9**) and deoxyviolacein (**10a-c**), as analysed by LC-HRMS/MS (**Table S2**). **(B)** Four constructs constituting various combinations of violacein and/or rebeccamycin biosynthetic genes to generate chlorinated violacein analogues. Pathway symbols were drawn using SBOL visual standard for biological parts. **(C)** Representative extracted ion chromatograms (EIC) targeting $[M+H]^+$ m/z of **1**, **2**, **9**,

10a-c detected from ethanol extracts of *E. coli* cells harbouring one of the pathway combinations in **(B)**. Compounds detected are shown with dotted line to indicate approximate retention times. Compounds **2** and **9** eluted at the same retention time. VioABCDE sample was run on a separate day so the retention time was slightly later than the other three samples. Peaks corresponding to other chlorinated compounds (**9**, **10a-c**) are too weak to be visible on the EIC. **(D)** Area under curves of m/z species extracted at the MS/MS level from TIC of ethanol extracts from cells harbouring respective pathway combination in B. Vio analogue refers to **9**, whereas DV analogues refer to **10a-c**. **(E)** Percentage compositions of Vio and DV analogues from different *E. coli* strains expressing hybrid Reb/Vio pathway variants. Data shows the mean and SD of biological duplicates. **(F)** Percentage compositions of 7-chloro analogues of violacein and deoxyviolacein extracted from *E. coli* expressing RebFHOD+VioCDE with different combinations of medium (J23108, green) and weak (J23114, grey) promoters controlling the expression of RebF, RebH and VioD. Data shows the mean and SD of biological triplicates.

Further derivatisation, through chemical cross-coupling, of new-to-nature, halogenated natural product analogues generated by a synthetic biological strain, was first demonstrated with pacidamycins (Deb Roy et al., 2010). We applied a similar strategy by first feeding 5-bromo-DL-tryptophan to *E. coli* cells expressing VioABCDE to generate 5'-bromo-violacein and 5'-bromo-deoxyviolacein which were detected by LC-HRMS/MS (**Table S2**). We then proceeded to screen a series of conditions that might facilitate Suzuki-Miyaura cross-coupling. However, due to low titres of 5'-bromo-violacein and 5'-bromo-deoxyviolacein available in the crude extract, and challenges relating to the separation of these compounds that showed propensity for pi-stacking, isolation of products for further characterisation and bioassays of the cross-coupling product proved difficult. We thus focused on systemically identifying conditions that would allow direct cross-coupling in crude extracts which identified optimal conditions for derivatization. The corresponding cross-coupling products 5'-(*p*-tolyl)-violacein and 5'-(*p*-tolyl)-deoxyviolacein were detected in the cross-coupling mixture by LC-HRMS/MS (**Figure 4A**, **Table S2**). Having identified the optimised conditions for cross-coupling at low concentrations, we performed cross-coupling reaction with a selection of 15 aryl boronic acids chosen to sample a wide range of steric and electronic variations, which gave a total of 20 new cross-coupled analogues of violacein and deoxyviolacein (**Figure 4B**). We observed that while boronic acids with electron-donating groups (*e.g. p*-methoxyphenylboronic acid) gave better yield and MS/MS data were obtained, for those with electron-withdrawing groups (*e.g. p*-formylphenylboronic acid), only MS data were obtained due to lower conversion and more difficult electrospray ionisation of corresponding violacein analogues (**Table S2**). Pleasingly,

even boronic acid pinacol esters were successfully converted into the corresponding violacein product (*e.g. p*-cyanophenylboronic acid pinacol ester). In summary, the optimised conditions showed that a variety of cross-coupling analogues could be synthesised without the need for purification prior to cross-coupling, allowing for rapid access to potential cross-coupling products.

A

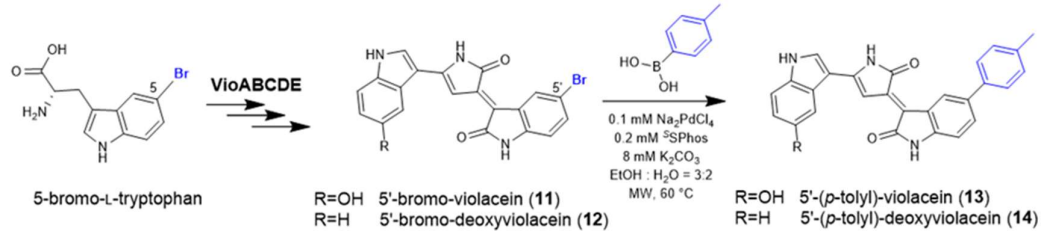

B

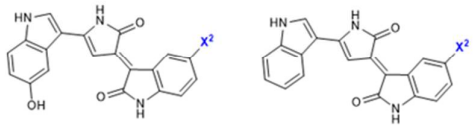

Compound number

X^2	Violacein derivative	Deoxyviolacein derivative
	13	**14**
	ND	**54**
	ND	**55**
	56	**57**
	58	**59**
	ND	**60**
	61	**62**
	63	**64**
	ND	**65**
	66	**67**
	68	ND
	69	**70**
	ND	**71**

C

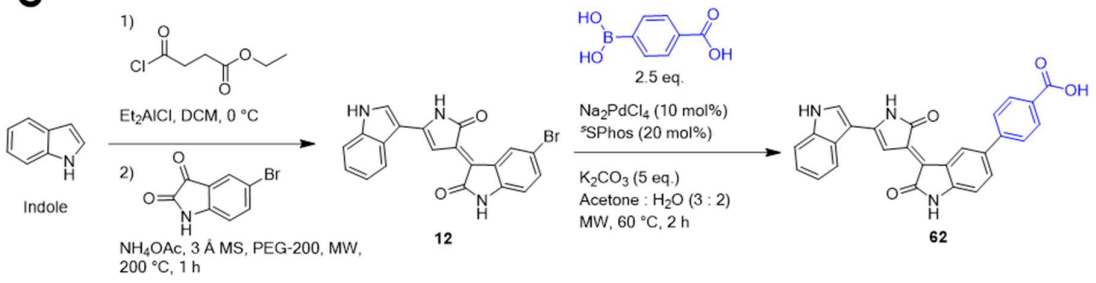

Figure 4. Further derivatisation of violacein and deoxyviolacein analogues via Suzuki-Miyaura cross-coupling reactions directly in crude extracts. **(A)** Optimised conditions for cross-coupling reaction directly in crude extracts. Coupling partner indicated is *p*-tolyl-boronic acid. **(B)** Compound numbers of full range of cross-coupled products as detected by LC-HRMS or LC-HRMS/MS (see **Table S2**). ND, not detected. **(C)** Starting from indole, 5'-bromo-deoxyviolacein (**12**) was synthesised in two steps, and used for preparative scale cross-coupling to afford the product (**62**) which was isolated and characterised by ^{1}H NMR analysis.

The attempts to isolate brominated violaceins, from the cell culture extracts, proved challenging due to low titres of desired compounds and co-elution as mixtures during chromatographic purifications. Hence, we decided to synthesise 5'-bromo-deoxyviolacein (**12**), which will be useful as a synthetic standard and for preparative scale cross-coupling reaction. To this end, we adapted a two-step protocol reported for synthesis of violacein analogues (McLaughlin et al., 2014). The condensation of the 3-acylated intermediate with 5-bromo-isatin proved challenging due to formation of a mixture of products. However, the desired product **12** was obtained in a 15% yield after two difficult chromatographic purification steps, further highlighting the benefits of the engineered biosynthesis. The LC retention time and LC-HRMS/MS analysis of the synthetic product matched with the biosynthetic **12,** and confirmed the identity as depicted. Furthermore, cross-coupling of synthetic **12** with *p*-carboxyphenylboronic acid proceeded with >70% yield based on LC-HRMS analysis; the product **62** was isolated (41% yield) from the crude reaction by extractive work-up (**Figure 4C**). The product was characterised by NMR and LC-HRMS analysis (**SI NMR Data**). These cross-coupling conditions provide a route to generating a diverse library of violacein analogues.

Significance

Combining the strengths of biosynthesis and organic synthesis, our GenoChemetic approach in generating diverse compounds has proven fruitful in exploring chemical space of natural products and their derivatives. In this study, inspection of the biosynthetic assembly of violacein and crystal structure analyses of the first enzyme L-tryptophan oxidase VioA suggested that various tryptophan substrate analogues could be enzymatically processed. We utilized this finding and designed experiments combining biosynthesis and chemical synthesis

to enable rapid access to 68 new violacein and deoxyviolacein analogues, in which only one (oxyviolacein) had been described previously. Furthermore, we have expanded this collection of compounds further via Suzuki-Miyaura cross-coupling reactions exploiting a brominated analogue of violacein, accessing an additional series of 20 violacein or deoxyviolacein coupling products. The ability to carry out these synthetic diversifications selectively on the halometabolites as components of a crude cell extract is exciting, paving the way towards building more diverse libraries of analogues. Although an initial growth inhibition screen of *B. subtilis* using crude extracts showed little change in activity compared with extracts containing violacein and deoxyviolacein, the encouraging inhibition activity displayed against *P. falciparum* malarial parasite in a recent study could warrant further investigation in other pathogens of interest. Finally, the combination of synthetic chemistry with synthetic biology, provides a more sustainable approach with the potential for application towards generating analogues of natural products in order to access greater chemical diversity rapidly and predictably.

Acknowledgements

HEL was supported by an Imperial College President's PhD Scholarship. We thank UKRI EPSRC (EP/K038648/1, EP/L011573/1 to PSF) and the European Union's Seventh Framework Programme (FP7/2007–2013/ERC grant agreement no 614779 GenoChemetics to RJMG) for funding. AMCO receives funding from EPSRC CRITICAT, EP/L016419/1. The authors thank all staff involved in Diamond Light Source Beamline I04-1 for assistance in VioA crystal data collection.

Author Contributions

HEL, SJM, KMP, SVS, AMCO, RJMG and PSF designed the study, analysed the data, and wrote the manuscript. HEL performed experiments under guidance of SJM, KMP and PSF.

AMCO performed cross-coupling reactions under guidance of SVS and RJMG. RL prepared and characterised the synthetic 5'-bromo-deoxyviolacein. AMCO and SMC performed LC-HRMS/MS analysis. RMM assisted on VioA crystallography, data collection and structure refinement. All authors read and approved the final draft of the manuscript.

Resource Availability

Lead Contact

Enquiries and requests for resources and reagents should be corresponded to the Lead Contact, Paul S. Freemont (p.freemont@imperial.ac.uk).

Materials Availability

Plasmids and strains generated from this study will be made available by the Lead Contact upon reasonable request.

Data and Code Availability

The authors declare that data supporting findings in this study is included in this paper and Supplemental Information. Sequences of plasmids used for expressing the violacein and the rebeccamycin/violacein hybrid pathways are available in the Supplemental Information. Raw data for NMR and LC-HRMS/MS analyses are available upon request. This study did not generate code.

Declaration of Interests

The authors declare no competing financial interests.

Supplemental Information

Supplemental Information is supplied as a separate PDF and an Excel file (Table S2 – Violacein and deoxyviolacein analogues MSMS fragment analysis).

Methods / Experimental Procedures

Materials

Restriction enzymes (NEB), T4 DNA ligase (Promega), Phusion (Agilent) and Q5 DNA polymerase (NEB) were used for routine cloning. QIAprep Miniprep Kit (Qiagen) and Zymoclean Gel DNA Recovery Kit (Zymogen) were used for plasmid extraction and purification. All chemicals, including tryptophan analogues, were purchased from either Sigma-Aldrich, Fluorochem or Acros Organics. All tryptophan analogues used are DL-racemic mixtures except L-tryptophan and 5-hydroxy-L-tryptophan. Primers were synthesized by Integrated DNA Technologies and sequencing was performed by Eurofins Genomics. Chemically competent DH10B (NEB) or JM109 (Promega) *Escherichia coli* strains were used for plasmid maintenance, cloning and expression of pathway enzymes. Depending on the plasmid antibiotic resistance marker, LB broth supplemented by carbenicillin (50 *µ*g/mL), chloramphenicol (35 *µ*g/mL) and kanamycin (50 *µ*g/mL) was used unless stated otherwise.

Constructing Rebeccamycin/Violacein hybrid pathway

The sequences of Rebeccamycin and Violacein pathway genes are available from the UniProt database. Violacein genes were PCR-amplified from Bba_K274002 plasmid (iGEM Parts Registry), adding NdeI and BamHI sites on the 5' and 3' ends respectively. RebF (Q8KI76), RebH (Q8KHZ8), RebO (Q8KHS0) and RebD (Q8KHV6) were synthesised commercially (GeneArt, Thermo Fisher) and cloned into appropriate pBP-ORF vector between NdeI and BamHI sites. Assembly variants of either the violacein pathway (pTU2S(VioAE)-b-VioBCD) or the violacein/rebeccamycin hybrid pathway (pTU2-A-RebOD-VioCDE, pTU2S(VioABEDC)-a-RebFH and pTU3-A-RebFHOD-VioCDE-KanR) were constructed using a modular cloning toolkit EcoFlex[22], and most of the genetic parts are available on Addgene (Kit #1000000080). Briefly, all genes, including a kanamycin resistance marker KanR, were cloned into holding vector pBP-ORF, and then assembled into individual transcription units with defined promoters (BBa_J23114, BBa_J23108, SJM932, SJM933, SJM935, T7-RBS-His), pET-RBS and terminators (BBa_B0015, L2U2H09, L2U5H08 and L3S2P21). For full assembly protocol please refer to **SI Protocol**. Plasmid and protein sequences are available in **SI Appendices**.

Culture growth and violacein extraction protocol

For test cultures to check for presence of novel analogues, typically 10 mL of autoclaved LB media in 50 mL sterile tubes were used. *E. coli* JM109 strain (Promega) harbouring the violacein pathway plasmid (pTU2S(VioAE)-b-VioBCD) was inoculated into overnight culture, which was then diluted 1:100 with fresh media and grown for 4 to 6 hours at 37 ºC until reaching OD 0.5, and 0.04% (w/v) tryptophan analogue (dissolved in 0.5 M HCl) and equal volume of 0.5 M NaOH were added. Cultures were then incubated at 25 °C for up to 65 hours. Cells were harvested by centrifugation (4000 x *g*, 4 °C, 10 min) and supernatant was removed. For each 10 mL of culture grown, 1 mL of ethanol was added to the cell pellet, and the mixture was transferred into smaller tubes and incubated at 75 °C for about 30 min, or until cell pellet turns greyish-white. The mixture was then centrifuged (15,000 x *g*, RT, 1 min) and the supernatant transferred to fresh tube for storage at -20 °C or diluted 1:50 with ethanol for injection into LC-HRMS/MS for detection of analogues. For long-term storage, the ethanol extract was dried down under vacuum and resuspended in DMSO, and then stored at -20 °C. Concentration was measured by comparing absorbance at 575 nm using purified violacein (Sigma) as calibration standards.

VioA purification and crystallisation

The *vioA* gene was amplified and cloned between NdeI and BamHI sites of pET-15b expression vector (Novagen) which contained an N-terminal hexahistidine tag. The vector was transformed into BL21 DE3 pLysS *Escherichia coli* (NEB) strain, grown in 1 L LB broth supplemented with 50 *µ*g/mL ampicillin at 37 °C until OD_{600} reached 0.6, and then induced with 0.2 mM IPTG and further incubation at 20 °C for 18 hours. Cells were then pelleted by centrifugation (4k rpm, 4 °C, 20 min) and resuspended in Binding Buffer (20 mM Tris pH 8,

500 mM NaCl, 10 mM Imidazole). Cells were sonicated (2 s on 2 s off at 70% amplitude for 4 min) and cell debris pelleted by centrifugation (15k rpm, 4 °C, 30 min). The supernatant was subjected to affinity purification by injecting into HisTrap HP column (GE Healthcare), with Buffer A as Binding Buffer and Buffer B as Elution Buffer (20 mM Tris pH 8, 500 mM NaCl, 500 mM Imidazole). Elution fractions were checked with SDS-PAGE, and fractions containing most VioA (49 kDa) were pooled and concentrated with Amicon Ultra-15 10K MWCO concentrator (EMD Millipore) and desalted with PD-10 Desalting Column (GE Healthcare) into GF Buffer (20 mM CHES pH 9.0, 25 mM NaCl). Protein solution was then subjected to SEC by injecting into HiLoad 16/60 Superdex 200 column (GE Healthcare) equilibrated with GF Buffer. Peak fractions were pooled and concentrated to 5 mg mL^{-1} measured on spectrophotometer with molar extinction coefficient from ProtParam (ExPASy). Concentrated proteins were then screened initially with sparse matrix (Crystal Screen 1 & 2 from Hampton Research), and hit condition was optimized in 24-well sitting drop plates with protein-to-buffer ratio 2:1. The best crystals were obtained with 100 mM HEPES pH 7.5, 9% PEG 8000 and 9% ethylene glycol incubated at 20 ˚C.

Horseradish peroxidase-coupled VioA kinetic assay

The Infrared Fluorimetric Hydrogen Peroxide Assay Kit (Sigma-Aldrich #MAK166) was used for VioA kinetic assays. In each reaction well in 96-well plate, 50 *μ*L of 2X master mix (infrared peroxidase substrate, final concentration 0.4 U/mL horseradish peroxidase in 100 mM CHES pH 9 buffer) was added to 25 *μ*L tryptophan (TRP, 4FT, 5MeT, 6FT and 7MeT, diluted with 100 mM CHES pH 9 buffer) such that final concentrations would range from 2.4 *μ*M to 5 mM. The reaction is then initiated by injecting 25 *μ*L of VioA (final concentration 25 nM) in 100 mM CHES pH 9 buffer into each well (total volume per reaction is 100 *μ*L) and fluorescence is monitored for 30 s at 1-second intervals using 640/680 nm as excitation/emission wavelengths, with temperature maintained at 25 °C. A hydrogen peroxide standard calibration curve was also determined by adding 50 *μ*L of 2X master mix to 50 *μ*L hydrogen peroxide of known concentrations, incubated in the dark for 1 minute, and measured at the same conditions as above. Linear regression analysis was used to determine the slopes of linear region, and the slopes were used to fit either Michaelis-Menten model (4FT) or Substrate inhibition model (TRP, 5MeT, 6FT, 7MeT) to calculate the best-fit values and standard errors of k_{cat}, K_M and K_i (where applicable) in GraphPad Prism 8.0.1.

Determination of apo VioA and tryptophan-bound VioA structures

VioA crystal was fished and cryoprotected with 20% ethylene glycol, and then snap frozen in liquid nitrogen before sending to Diamond Light Source for X-ray diffraction. Tryptophan-soaked crystals (L-tryptophan, 4-fluoro-DL-tryptophan, 5-methyl-DL-tryptophan, 6-fluoro-DL-tryptophan and 7-methyl-DL-tryptophan) were prepared by immersing crystal in mother liquor with added respective 1 mM L-tryptophan or 2 mM racemic tryptophan analogues for 30 minutes at room temperature. Datasets collected from DLS (i04-1 or i03 beamlines) were processed with in-house DIALS/Xia2 algorithm, and phase information was solved by PHASER (McCoy et al., 2007) molecular replacement with a model structure with PDB ID **3X0V** (L-lysine oxidase, 17% sequence identity). Further rounds of refinement and model building was done in Phenix (Adams et al., 2010) and *Coot* (Emsley et al., 2010) respectively (see **Table S1** for data collection and refinement statistics). L-tryptophan and its analogues-bound VioA structures were solved using molecular replacement with the apoenzyme structure as model. Protein structures are visualized using PyMOL Molecular Graphics System, Version 1.8 Schrödinger, LLC.

LC-HRMS/MS analyses of violacein analogues

Violacein analogues were detected by Agilent 1290 LC and 6550 Q-ToF mass spectrometer with electrospray ionization, using Agilent Zorbax Extend C-18 column (2.1 x 50 mm, 1.8 *μ*m particle size). For LC, buffer A was water with 0.1% (v/v) formic acid and buffer B was acetonitrile with 0.1% (v/v) formic acid, for total running time of 13 minutes including 3 min post-run time. 2 *μ*L diluted samples were injected, and the column was washed at 0.35 ml/min

with the following gradient: 0 min 5% B, 1 min 5% B, 9 min 70% B, 10 min 70% B. Quantification was by peak area of integrated chromatograms at targeted $[M+H]^+$ mass with ±20 ppm window. The protonated molecules of each analyte, $[M+H]^+$, were targeted and subjected to collision-induced dissociation (collision energy 30 eV), with product ions accumulated throughout the analysis. In calculating percentage composition of analogues, all compounds were assumed to have the same mass response as there is no mass spectrometry standard available for every compound detected.

Growth inhibition bioassays against *B. subtilis*

100 μL overnight culture of *B. subtilis* is inoculated into 6 mL of fresh LB and grown for ~3 h until OD600 reaches around 0.3 to 0.5. In the meantime, serial dilutions of crude violacein extracts were prepared with DMSO to obtain a range of concentrations between 1 to 10 ng/μL. Concentration of crude violacein extract stocks were calibrated against Violacein standard (Sigma) using absorbance at 575 nm. 16.5 μL of crude violacein extract at each concentration is added to 313.5 μL of *B. subtilis* culture diluted with fresh LB to OD 0.1 to adjust final concentration of drugs to 0.05 to 0.5 ng/μL while keeping DMSO concentration constant at 5% (w/v). 100 μL of mixture was then transferred in triplicate wells in a 96-well flat-bottom plate (Greiner), and Breathe-easy sealing membrane (Sigma) was applied to minimize liquid evaporation and allow gaseous exchange. *B. subtilis* culture with 5% DMSO (without drug) was also prepared as negative control. The OD was measured at 600 nm at 10 min intervals over 18 hours, and the incubation chamber temperature was set at 30 °C throughout. Experiments were performed on three separate days to obtain biological triplicates. Endpoint (18 h) OD600 values were normalised against negative control and plotted against drug concentration. Non-linear regression fit analysis was performed using GraphPad Prism version 7.03 for Windows, GraphPad Software, La Jolla California USA, www.graphpad.com. Specifically, the inhibitor concentration vs response - variable slope (four parameters) with robust fitting method was chosen, and IC50 and their associated RSDR (Robust Standard Deviation of the Residuals) values were obtained from the analysis and plotted for each crude violacein extract tested.

Generation and extraction of brominated violacein analogues

E. coli JM109 cells (comprising *vioABCDE* genes) were cultured in TB media (1 L in 2 L flask) at 37 °C for 9 hours until OD600 reaches 0.4-0.6. Commercial 5-bromo-DL-tryptophan (Sigma) was added (1 mM final concentration) and cultures were further incubated for at 25 °C for 2 days. Cells were harvested by centrifugation (4000 rpm, 20 min) and stored at -20 °C. For extraction, 30 mL ethanol was added to 4 mL of *E. coli* frozen pellets containing brominated violacein, and the solution was stirred (500 rpm) at 50 °C for 1 hour. After cooling to room temperature, the extract was centrifuged (3000 rpm, 10 mins) and the supernatant crude extract containing violacein species were aliquoted (1 mL) and stored at -20 °C.

Cross-coupling of brominated violacein from crude extract and LC-HRMS/MS analysis

In a glass microwave vial, Na_2PdCl_4 (100 μL, 1mM stock in water) and ^{S}SPhos (100 μL, 2 mM stock in water) were mixed for 5 minutes in ethanol (300 μL). Then, freshly prepared solution of appropriate boronic acid (200 μL, 20 mM stock in ethanol), K_2CO_3 (200 μL, 40 mM stock in water) and crude violacein extract (100 μL in ethanol) were sequentially added, so the final concentration of ethanol was 60%. The vial was sealed and heated in a microwave reactor at 60 °C for 2 hours (microwave reactions were carried out using Biotage Initiator+ in appropriate Biotage Microwave Vials sealed with aluminium crimp caps). The palladium was then quenched with a solution of DTT (1:1 volume, 200 mM in water) and left stirring for 30 minutes. The solution was finally diluted by 5-fold (1:1 water:ethanol), centrifuged (13000 rpm, 10 min) and clear supernatant was analysed by LC-HRMS/MS. High resolution mass spectra were recorded on a Waters Micromass LCT time of flight mass spectrometer coupled to a Waters 2975 HPLC system or an Orbitrap VELOS pro. Data analysis was performed with Thermo Xcalibur 3.0.63.3 software. Samples were prepared in a 1:1 mixture of methanol water and

injected with a 100 μL syringe. The solvent system consisted of 0.1% formic acid in water (A) and acetonitrile (B). Products were eluted using a standard gradient from 5% B to 100% B over 15 minutes with a flow rate of 0.35 mL/min. The column used was a Kinetex 2.6 μm EVO C18 100 Å, LC Column 100 x 2.1 mm.

Synthesis of 5'-bromo-deoxyviolacein (**12**)

Step 1: Indole (586 mg, 5.0 mmol, 1.0 eq.) was dissolved in dichloromethane in a 3-necked flask and cooled to 0 °C, the flask was flushed with argon and sealed with a Suba-Seal. To this was added Et_2AlCl (7.5 mL, 7.5 mmol, 1.5 eq.) as a 1.0 M solution in hexanes, via syringe through the seal. The resulting mixture was stirred at 0 °C for 25 mins. After this time the ethyl-4-chloro-4-oxobutyrate was added slowly (over 5 mins) via syringe through the seal, maintaining the reaction temperature between 0 and 2 °C. The reaction mixture was stirred for a further 2 hours allowing warming to room temperature. The resulting dark red solution was quenched by slowly adding NH_4Cl (Sat. aq.) (5 mL). Water was added to the resulting suspension and this was then extracted with ethyl acetate, washed with Rochelle's salt twice, washed $NaHCO_3$ (aq.) twice and dried over magnesium sulfate, then filtered and evaporated *in vacuo* to give a pale-yellow solid. The solid was further purified by flash chromatography eluting gradient 20-70% ethyl acetate in hexane to give yellow solid 0.58 g, 47% yield. **^{1}H NMR (500 MHz, $CDCl_3$)** δ 8.60 (s, 1H), 8.42 – 8.34 (m, 1H), 7.92 (d, *J* = 3.0 Hz, 1H), 7.46 – 7.39 (m, 1H), 7.32 – 7.28 (m, 2H), 4.17 (q, *J* = 7.1 Hz, 2H), 3.24 (t, *J* = 6.9 Hz, 2H), 2.80 (t, *J* = 6.9 Hz, 2H), 1.27 (t, *J* = 7.1 Hz, 3H). **^{13}C NMR (126 MHz, $CDCl_3$)** δ 194.0 (C=O), 173.9 (C=O), 136.5 (C_{arom}), 131.8 (CH_{arom}), 125.5 (C_{arom}), 123.7 (CH_{arom}), 122.7 (CH_{arom}), 122.2 (CH_{arom}), 117.4 (C_{arom}), 111.7 (CH_{arom}), 60.9 (CH_2), 34.1 (CH_2), 28.6 (CH_2), 14.3 (CH_3). **HRMS (ESI+)** *m/z* calculated for $C_{14}H_{16}NO_3$ $[M+H]^+$ 246.1125, found 246.1122.

Step 2: Above intermediate (50 mg, 0.203 mmol, 1.0 eq.) was weighed into a MW vial, followed by 3Å molecular sieves (pre-dried, 260 mg), 5-bromo-isatin (53 mg, 0.23 mmol, 1.15 eq.), NH_4OCOMe (79 mg, 0.815 mmol, 4.0 eq.) and PEG-200 (1.5 mL, pre-dried over 3Å molecular sieves for 24 hours). The vial was sealed and then evacuated and filled with argon 3 times and stirred at room temperature for 30 mins. The sealed vial was then heated in the microwave at 200 °C for 3 hours. The resulting dark blue solution was diluted with water and ethyl acetate forming an emulsion, brine was added to break the emulsion and the mixture was extracted with ethyl acetate, organic layers were combined and washed with brine and then dried over magnesium sulfate. The resulting purple solid was further purified by flash chromatography 10-100% ethyl acetate in hexane. The bromo-violacein enriched material was further purified by HPLC reversed phase C_{18} column (Kinetex® 5 µm EVO C18 100 Å, 250x10.0 mm) on an HPLC, eluting with water (containing 0.1% formic acid) and acetonitrile. Starting conditions at 25% acetonitrile, with a one-hour gradient to 50% acetonitrile. Purple fractions were collected and combined to yield 5'-bromo-deoxyviolacein **12** (12 mg, 15% yield). **^{1}H NMR (500 MHz, Acetone-d_6)** δ 11.39 (s, 1H), 9.89 (s, 1H), 9.82 (s, 1H), 9.31 (d, *J* = 2.0 Hz, 1H), 8.29 – 8.22 (m, 1H), 8.05 – 7.93 (m, 1H), 7.86 (d, *J* = 2.0 Hz, 1H), 7.61 (dd, *J* = 6.6, 1.8 Hz, 1H), 7.38 (dd, *J* = 8.3, 2.1 Hz, 1H), 7.36 – 7.31 (m, 1H), 6.90 (d, *J* = 8.3 Hz, 1H), 5.62 (s, 1H). **HRMS (ESI$^+$)** *m/z* calculated for $C_{20}H_{13}BrN_3O_2$ $[M+H]^+$ 406.0186, found 406.0182.

Cross-coupling of synthetic **12** on preparative scale

In a glass microwave vial, Na_2PdCl_4 (100 µL from 5 mM stock solution, 10 mol%) and ^{S}SPhos (100 µL from 10 mM stock solution, 20 mol%) were mixed for 5 minutes in water:acetone (1:1, 400 µL). Then a freshly prepared solution of *p*-carboxyphenylboronic acid (200 µL from 60 mM stock solution in ethanol, 12.3 µmol, 2.5 eq.) was added followed by K_2CO_3 (3.4 mg, 24.6 µmol, 5 eq.) and 5'-bromo-deoxyviolacein (**12**) (2 mg, 4.9 mmol, in 200 µL of acetone, 1 eq.). The vial was sealed and heated at 60 °C for 2 hours in a microwave reactor. The yield was estimated to be >70% from LC-MS analysis. The solvent was removed under vacuum. The solid was washed with ethanol, before being partially solubilised in acetone. The acetone was transferred to a clean vial and dried under vacuum, to afford 5'-(*p*-carboxyphenyl)-

deoxyviolacein **62** (0.9 mg, 41% yield). **^{1}H NMR (500 MHz, Acetone-d_6)** δ 9.32 (d, *J* = 2.0 Hz, 1H), 8.28 (s, 1H), 8.17 (d, *J* = 8.5 Hz, 1H), 8.04 (m, 1H), 8.01 (d, *J* = 7.6 Hz, 1H), 7.91 (d, *J* = 8.8 Hz, 1H), 7.90 (s, 1H), 7.62 (m, 2H), 7.52 (t, *J* = 7.7 Hz, 1H), 7.40 (d, *J* = 2.1 Hz, 1H), 7.38 (d, *J* = 2.0 Hz, 1H), 7.35 (m, 2H), 6.92 (d, *J* = 8.8 Hz, 1H), 6.89 (d, *J* = 8.2 Hz, 1H). **HRMS (ESI$^+$)** *m/z* calculated for $C_{27}H_{18}N_3O_4$ $[M+H]^+$ 448.1292, found 448.1286.

References

Adams, P.D., Afonine, P.V., Bunkóczi, G., Chen, V.B., Davis, I.W., Echols, N., Headd, J.J., Hung, L.-W., Kapral, G.J., Grosse-Kunstleve, R.W., et al. (2010). PHENIX: a comprehensive Python-based system for macromolecular structure solution. Acta Crystallogr. D Biol. Crystallogr. *66*, 213–221.

Balibar, C.J., and Walsh, C.T. (2006). In vitro biosynthesis of violacein from L-tryptophan by the enzymes VioA-E from Chromobacterium violaceum. Biochemistry *45*, 15444–15457.

Bilsland, E., Tavella, T.A., Krogh, R., Stokes, J.E., Roberts, A., Ajioka, J., Spring, D.R., Andricopulo, A.D., Costa, F.T.M., and Oliver, S.G. (2018). Antiplasmodial and trypanocidal activity of violacein and deoxyviolacein produced from synthetic operons. BMC Biotechnol. *18*, 22.

Deb Roy, A., Grüschow, S., Cairns, N., and Goss, R.J.M. (2010). Gene expression enabling synthetic diversification of natural products: chemogenetic generation of pacidamycin analogs. J. Am. Chem. Soc. *132*, 12243–12245.

Du, Y.-L., and Ryan, K.S. (2015). Expansion of bisindole biosynthetic pathways by combinatorial construction. ACS Synth. Biol. *4*, 682–688.

Durán, M., Ponezi, A.N., Faljoni-Alario, A., Teixeira, M.F.S., Justo, G.Z., and Durán, N. (2012). Potential applications of violacein: a microbial pigment. Med. Chem. Res. *21*, 1524–1532.

Eichner, S., Knobloch, T., Floss, H.G., Fohrer, J., Harmrolfs, K., Hermane, J., Schulz, A., Sasse, F., Spiteller, P., Taft, F., et al. (2012). The interplay between mutasynthesis and semisynthesis: generation and evaluation of an ansamitocin library. Angew. Chem. Int. Ed Engl. *51*, 752–757.

Emsley, P., Lohkamp, B., Scott, W.G., and Cowtan, K. (2010). Features and development of Coot. Acta Crystallogr. D Biol. Crystallogr. *66*, 486–501.

Eustáquio, A.S., Gust, B., Li, S.-M., Pelzer, S., Wohlleben, W., Chater, K.F., and Heide, L. (2004). Production of 8'-halogenated and 8'-unsubstituted novobiocin derivatives in genetically engineered streptomyces coelicolor strains. Chem. Biol. *11*, 1561–1572.

Füller, J.J., Röpke, R., Krausze, J., Rennhack, K.E., Daniel, N.P., Blankenfeldt, W., Schulz, S., Jahn, D., and Moser, J. (2016). Biosynthesis of Violacein, Structure and Function of l-Tryptophan Oxidase VioA from Chromobacterium violaceum. J. Biol. Chem. *291*, 20068–20084.

Goss, R.J.M., Shankar, S., and Fayad, A.A. (2012). The generation of "unnatural" products: synthetic biology meets synthetic chemistry. Nat. Prod. Rep. *29*, 870–889.

Haun, M., Pereira, M.F., Hoffmann, M.E., Joyas, A., Campos, V., Filardi, L.D., de Castro, S.L., and Duran, N. (1992). Bacterial chemistry. VI. Biological activities and cytotoxicity of 1,3-dihydro-2H-indol-2-one derivatives. Biol. Res. *25*, 21–25.

Heide, L., Westrich, L., Anderle, C., Gust, B., Kammerer, B., and Piel, J. (2008). Use of a halogenase of hormaomycin biosynthesis for formation of new clorobiocin analogues with 5-chloropyrrole moieties. Chembiochem *9*, 1992–1999.

Hoshino, T., and Ogasawara, N. (1990). Biosynthesis of Violacein: Evidence for the Intermediacy of 5-Hydroxy- l -tryptophan and the Structure of a New Pigment, Oxyviolacein, Produced by the Metabolism of 5-Hydroxytryptophan. Agric. Biol. Chem. *54*, 2339–2346.

Jeschek, M., Gerngross, D., and Panke, S. (2016). Rationally reduced libraries for combinatorial pathway optimization minimizing experimental effort. Nat. Commun. *7*, 11163.

Jiang, P.-X., Wang, H.-S., Xiao, S., Fang, M.-Y., Zhang, R.-P., He, S.-Y., Lou, K., and Xing, X.-H. (2012). Pathway redesign for deoxyviolacein biosynthesis in Citrobacter freundii and characterization of this pigment. Appl. Microbiol. Biotechnol. *94*, 1521–1532.

Jones, J.A., Vernacchio, V.R., Lachance, D.M., Lebovich, M., Fu, L., Shirke, A.N., Schultz, V.L., Cress, B., Linhardt, R.J., and Koffas, M.A.G. (2015). ePathOptimize: A Combinatorial Approach for Transcriptional Balancing of Metabolic Pathways. Sci. Rep. *5*, 11301.

Kirschning, A., and Hahn, F. (2012). Merging chemical synthesis and biosynthesis: a new chapter in the total synthesis of natural products and natural product libraries. Angew. Chem. Int. Ed Engl. *51*, 4012–4022.

Kufs, J.E., Hoefgen, S., Rautschek, J., Bissell, A.U., Graf, C., Fiedler, J., Braga, D., Regestein, L., Rosenbaum, M.A., Thiele, J., et al. (2020). Rational design of flavonoid production routes using combinatorial and precursor-directed biosynthesis. ACS Synth. Biol. *9*, 1823–1832.

Lai, H.-E., Moore, S., Polizzi, K., and Freemont, P. (2018). EcoFlex: A Multifunctional MoClo Kit for E. coli Synthetic Biology. In Synthetic Biology: Methods and Protocols, J.C. Braman, ed. (New York, NY: Springer New York), pp. 429–444.

McCoy, A.J., Grosse-Kunstleve, R.W., Adams, P.D., Winn, M.D., Storoni, L.C., and Read, R.J. (2007). Phaser crystallographic software. J. Appl. Crystallogr. *40*, 658–674.

McLaughlin, E.C., Norman, M.W., Ko Ko, T., and Stolt, I. (2014). Three-component synthesis of disubstituted 2H-pyrrol-2-ones: preparation of the violacein scaffold. Tetrahedron Lett. *55*, 2609–2611.

Moore, S.J., Lai, H.-E., Kelwick, R.J.R., Chee, S.M., Bell, D.J., Polizzi, K.M., and Freemont, P.S. (2016). EcoFlex: A Multifunctional MoClo Kit for E. coli Synthetic Biology. ACS Synth. Biol. *5*, 1059–1069.

Nishizawa, T., Grüschow, S., Jayamaha, D.-H.E., Nishizawa-Harada, C., and Sherman, D.H. (2006). Enzymatic assembly of the bis-indole core of rebeccamycin. J. Am. Chem. Soc. *128*, 724–725.

Okano, A., Isley, N.A., and Boger, D.L. (2017). Peripheral modifications of [Ψ[CH2NH]Tpg4]vancomycin with added synergistic mechanisms of action provide durable and potent antibiotics. Proc. Natl. Acad. Sci. U. S. A. *114*, E5052–E5061.

Petersen, M.T., and Nielsen, T.E. (2013). Tandem ring-closing metathesis/isomerization reactions for the total synthesis of violacein. Org. Lett. *15*, 1986–1989.

Richter, M.F., Drown, B.S., Riley, A.P., Garcia, A., Shirai, T., Svec, R.L., and Hergenrother, P.J. (2017). Predictive compound accumulation rules yield a broad-spectrum antibiotic. Nature *545*, 299–304.

Runguphan, W., Qu, X., and O'Connor, S.E. (2010). Integrating carbon-halogen bond formation into medicinal plant metabolism. Nature *468*, 461–464.

Sánchez, C., Zhu, L., Braña, A.F., Salas, A.P., Rohr, J., Méndez, C., and Salas, J.A. (2005). Combinatorial biosynthesis of antitumor indolocarbazole compounds. Proc. Natl. Acad. Sci. U. S. A. *102*, 461–466.

Wang, H., Wang, F., Zhu, X., Yan, Y., Yu, X., Jiang, P., and Xing, X.-H. (2012). Biosynthesis and characterization of violacein, deoxyviolacein and oxyviolacein in heterologous host, and their antimicrobial activities. Biochem. Eng. J. *67*, 148–155.

Wilkinson, M.D., Lai, H.-E., Freemont, P.S., and Baum, J. (2020). A Biosynthetic Platform for Antimalarial Drug Discovery. Antimicrob. Agents Chemother. *64*.

Wille, G., and Steglich, W. (2001). A Short Synthesis of the Bacterial Pigments Violacein and Deoxyviolacein. Synthesis *2001*, 0759–0762.

Yamaguchi, H., Tatsumi, M., Takahashi, K., Tagami, U., Sugiki, M., Kashiwagi, T., Kameya, M., Okazaki, S., Mizukoshi, T., and Asano, Y. (2018). Protein engineering for improving the thermostability of tryptophan oxidase and insights from structural analysis. J. Biochem. *164*, 359–367.

Yeh, E., Garneau, S., and Walsh, C.T. (2005). Robust in vitro activity of RebF and RebH, a two-component reductase/halogenase, generating 7-chlorotryptophan during rebeccamycin biosynthesis. Proc. Natl. Acad. Sci. U. S. A. *102*, 3960–3965.

Yeh, E., Blasiak, L.C., Koglin, A., Drennan, C.L., and Walsh, C.T. (2007). Chlorination by a long-lived intermediate in the mechanism of flavin-dependent halogenases. Biochemistry *46*, 1284–1292.

Zalatan, J.G., Lee, M.E., Almeida, R., Gilbert, L.A., Whitehead, E.H., La Russa, M., Tsai, J.C., Weissman, J.S., Dueber, J.E., Qi, L.S., et al. (2015). Engineering complex synthetic transcriptional programs with CRISPR RNA scaffolds. Cell *160*, 339–350.